

# Blends of poly(ethylene oxide) and poly(4-vinylphenol-*co*-2-hydroxyethyl methacrylate): thermal analysis, morphological behaviour and specific interactions

Ana Maria Rocco\*, C.E. Bielschowsky, Robson Pacheco Pereira

*Grupo de Materiais Condutores, Instituto de Química, Universidade Federal do Rio de Janeiro, CT,  
Bloco A, Cidade Universitária, Rio de Janeiro 21945-970, Brazil*

Received 15 May 2002; received in revised form 15 October 2002; accepted 24 October 2002

## Abstract

DSC and optical microscopy were used to determine the miscibility and crystallinity of blends of poly(ethylene oxide) (PEO) with poly(4-vinylphenol-*co*-2-hydroxyethyl methacrylate) (PVPh-HEM). A single glass transition temperature was observed for all blends, indicating miscibility. A progressive decrease in the degree of crystallinity and in the size of the PEO spherulites is observed, as PVPh-HEM is added. FTIR was used to probe the intermolecular specific interactions of the blends and the miscibility of the blend is mainly attributed to PVPh-HEM/PEO intermolecular interactions via hydrogen bonding.

© 2002 Elsevier Science Ltd. All rights reserved.

**Keywords:** Blends; Miscibility; Poly(ethylene oxide)

## 1. Introduction

Polymer solid electrolytes (PSE) are materials of great technological interest because of their applications in solid-state batteries [1], capacitors [2] and electrochromic devices [3]. Polymer electrolyte materials are characterized by an interesting conductivity behaviour that is highly dependent on the local structure and is influenced by crystallization and ionic association. Among the first and most studied polymers for PSE is poly(ethylene oxide) PEO, due to the fact that it easily dissolves alkali metal salts. However, PEO possesses appreciable ionic conduction only above 65 °C, since ion conduction takes place primarily in the non-crystalline regions [4]. At temperatures below 65 °C, PEO-salt complexes consist of mixtures of spherulite crystalline phases, separated by amorphous solutions of salt in PEO [5].

One of the methods to improve the conductivity of PEO-based electrolytes is modification of the polymer matrix by incorporation of plasticizers, to make the matrix more liquid-like. The addition of small molecules, such as PEO oligomers, ethylene carbonate and propylene carbonate as plasticizers, facilitates long chain segmental motion.

However, a serious disadvantage is that most plasticizers are volatile at room temperature, leading to their loss from the samples [6]. Efforts to enhance the ionic conductivity of the solid electrolytes based on PEO focused on suppressing its crystallization, via incorporation of compounds with low glass transition temperatures ( $T_g$ ) [7], and by copolymerization of PEO with macromonomers [8]. Copolymerization is a way to lower the melting point, modulus as well as crystallinity and to increase solubility and transparency [9]. Possible alternatives are grafting [10] and cross-linking [11]. Although these novel approaches are promising, the fact that their preparation sometimes requires non-trivial synthetic processes is a serious drawback to practical applications. It is of considerable importance to develop an easier method for preparing the polymer electrolytes with higher ionic conductivities and dimensional stability. In this regard, recent works on the preparation of polymer electrolytes by blending polymers are of interest [12,13]. Blending polymers is an economic and quick alternative for obtaining materials with optimized properties. The main advantages of these blend-based systems are simplicity of preparation and easy control of physical properties by compositional change. Much work has been done on binary PEO-based blends, where the second component is non-crystalline and is able to inhibit crystallization of the PEO

\* Corresponding author. Fax: +55-21-2562-7559.

E-mail address: amrocco@iq.ufrj.br (A.M. Rocco).

[14–16]. Thermal, mechanical, and adhesive properties associated with high transparency, which are desirable for applications in devices, can be optimized by blending, depending on the non-crystalline polymer. These properties are optimized by casting on the electrodes, since this method allows one to obtain PSE films of less than 10  $\mu\text{m}$  thickness, which diminishes the time response of these devices [3].

Another important consideration in the choice of blend components is intermolecular interactions, which are considered to play a key role in polymer miscibility. It has been reported [17,18] that PEO, because of the presence of basic oxygen, is a good proton-accepting polymer, which permits a hydrogen-bonding interaction in a blend with a proton-donor polymer.

The main goal of this work is to obtain and characterize PEO/poly(4-vinylphenol-co-2-hydroxyethyl methacrylate) (PVPh-HEM) blends by its thermal, morphological and spectroscopic properties.

## 2. Experimental section

### 2.1. Materials

The PVPh-HEM (55 mol% in vinylphenol) and PEO ( $M_w = 4 \times 10^6$  g/mol) were supplied by Aldrich Chem. Co. and utilized without further purification. Methanol (Merck, PA) was distilled and stored under molecular sieves.

### 2.2. Sample preparation

PEO and PVPh-HEM with ratios of 100/0, 90/10, 80/20, 70/30, 60/40, 50/50, 40/60, 30/70, 20/80, 10/90 and 0/100 wt% were dissolved in methanol. The solution was stirred for 8 h. Films were prepared by casting from these solutions on to glass plates and drying at 35  $^{\circ}\text{C}$ , in a desiccator under vacuum. The samples were allowed to dry for 48 h to achieve constant weight.

### 2.3. Differential scanning calorimetry (DSC)

To evaluate the miscibility and thermal behaviour of the blends, DSC measurements were performed on a General V4.1C DuPont 2100 apparatus. The apparatus was calibrated with an indium standard under nitrogen atmosphere.

Samples were first heated from 25 to 100  $^{\circ}\text{C}$  at a heating rate of 10  $^{\circ}\text{C min}^{-1}$  (run I). After a 5 min isotherm, samples were then cooled to  $-100$   $^{\circ}\text{C}$  at the same rate (run II) and then heated at 10  $^{\circ}\text{C min}^{-1}$  to 100  $^{\circ}\text{C}$  (run III). Sample sizes were kept around 5 mg and all the DSC measurements were performed in sealed aluminium pans under a  $\text{N}_2$  flow rate of 50 ml/min. The melting temperatures ( $T_m$ ) and apparent melting enthalpy ( $\Delta H_m$ ) were determined from the DSC endothermic peaks on the second heating run. Glass transition temperatures,  $T_g$ , were estimated as the onset

temperature. The melting enthalpies and temperatures were derived from the area and the maximum of the endothermic peaks, respectively. The degree of crystallinity was calculated from the following equations:

$$\chi_{c,\text{blend}} = \frac{\Delta H_{m,\text{blend}}}{\Delta H_{\text{PEO}}^0} \quad (1)$$

$$\chi_{c,\text{PEO}} = \frac{\Delta H_{m,\text{PEO}}}{\Delta H_{\text{PEO}}^0} \quad (2)$$

where  $\Delta H_{m,\text{blend}}$  and  $\Delta H_{m,\text{PEO}}$  are the apparent melting enthalpies per gram of blend and of PEO present on the blend, respectively, and  $\Delta H_{\text{PEO}}^0$  is the heat of melting per gram of 100% crystalline PEO, 188  $\text{J g}^{-1}$  [19].

### 2.4. Morphological studies

Samples deposited on glass plates were analysed using an Olympus BX-50 polarized light optical microscopy (PLOM). A magnification of 100 $\times$  was used for all the photomicrographs.

### 2.5. Fourier transform infrared spectroscopy

Fourier transform infrared spectroscopy (FTIR, Nicolet-760) was used for investigating possible molecular interactions between the constituents in the range of 400–4000  $\text{cm}^{-1}$ . Spectra were obtained at room temperature with a resolution of 1  $\text{cm}^{-1}$ , a scan number of 128 and optimized gain for all samples. The samples were prepared by casting as thin films of uniform thickness and dried under vacuum directly on to KBr.

### 2.6. Quantitative determinations from FTIR spectra

The hydroxyl and carbonyl regions vary markedly with hydrogen bonding, allowing one to separate different contributions from ‘free’ (non-hydrogen bonded) and ‘bound’ (hydrogen bonded) hydroxyl forms. Assuming that only these two forms (free and bound) are distinguishable in infrared spectra, a deconvolution treatment was employed, using Gaussians as primitive functions, according to the similar mathematical treatment described earlier [20]. The total areas were then normalized and the ratio of free and associated forms were taken from the relative areas associated with each form. The humidity control was done by obtaining FTIR spectra of PEO samples prepared concomitantly and treated in the same manner as the samples of the blends.

## 3. Results and discussion

### 3.1. DSC

DSC curves recorded during the second heating scan are

shown in Fig. 1. One endothermic peak was found for the PEO-rich samples (PVPh-HEM up to 40 wt%) and it was associated with the melting of the crystalline phase. Samples with 50 wt% or higher PVPh-HEM do not exhibit the endothermic peak characteristic of melting of the crystalline PEO phase. A progressive decrease in the area of the endothermic peak is observed with the addition of PVPh-HEM, up to 40 wt% (60 wt% PEO), and an exothermic peak also observed for this sample was attributed to crystallization during the second heating scan. This exothermic peak indicates that the PEO present in the sample exhibits difficulty to crystallize during the cooling scan.

In Table 1  $\Delta H_m$ , degree of crystallinity  $\chi_{c,blend}$ ,  $\chi_{c,PEO}$ ,  $T_m$ ,  $T_g$ , glass transition width ( $\Delta T_g$ ) and heat capacity change during the glass transition ( $\Delta C_p$ ), for all samples are listed. The presence of 40 wt% PVPh-HEM causes a decrease of  $T_m$ , from 72 °C (pure PEO) to 64 °C. The  $T_m$  obtained, most likely, does not correspond to the equilibrium melting temperature, but rather reflects morphological aspects (crystal size, defects on the crystalline phase) and also thermodynamic aspects. Despite the influence of morphological analysis, it is evident that the tendency of the lowering of  $T_m$  with an increase of the PVPh-HEM concentration in the blends indicates miscibility.

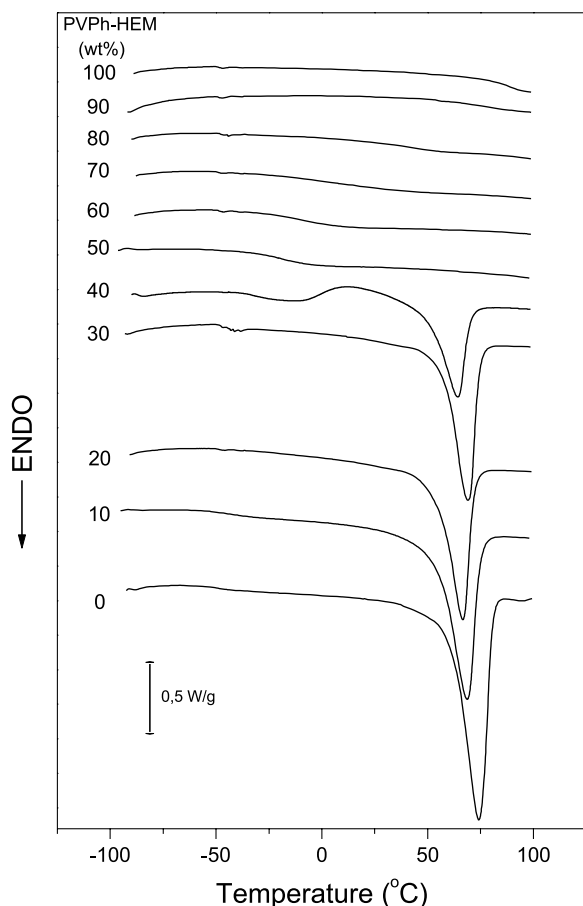


Fig. 1. DSC curves of PEO/PVPh-HEM blends.

Only one  $T_g$  can be observed for all of the samples, which indicates miscibility within the limits of detection of the DSC technique. The Fox equation (3) [21] and the Gordon–Taylor (G–T) model (Eqs. 4 and 5) [22] were utilized to describe the dependence of  $T_g$  on the composition of the blend (Fig. 2). These are empirical equations, which describe the dependence of  $T_g$  on the blend composition for miscible systems.

$$\frac{1}{T_g} = \frac{w_A}{T_{g,A}} + \frac{w_B}{T_{g,B}} \quad (3)$$

$$T_g = \frac{w_A T_{g,A} + K w_B T_{g,B}}{w_A + K w_B} \quad (4)$$

$$K = \frac{\Delta C_{p,A}}{\Delta C_{p,B}} \quad (5)$$

where  $w$  is mass percent of polymer A and B,  $T_g$  is glass transition for A and B polymers and  $K$  (Eq. 5) is the ratio of heat capacity change of PEO to that of PVPh-HEM [23].

The dependence of the calculated  $T_g$  on the blend composition exhibits a positive deviation from the Fox equation. This model describes the  $T_g$  behaviour for ideal mixtures, where it is assumed that the homogeneous and heterogeneous interactions are equivalent. The non-ideality of this system is expressed by deviations from the model and in the present work a positive deviation is probably caused by strong intermolecular interactions [24].

For the G–T model,  $K$  was calculated using Eq. 5 and its value was 0.198. Although some authors suggest that a low value of  $K$  indicates weak molecular interactions, the G–T model makes only thermal predictions [25]. The experimental  $T_g$  values shown in Fig. 2 are obviously strongly influenced by compositional changes and present good agreement with the model. A comparison of the experimental results with the G–T model suggests good homogeneity in the blend [26].

The  $\Delta T_g$  is defined as the difference between onset and endset of the glass transition process and reflects the number

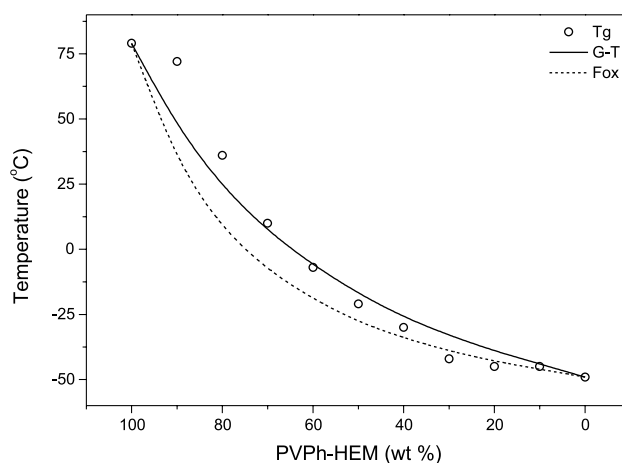


Fig. 2. Dependence of  $T_g$  of the PEO/PVPh-HEM blends on the PVPh-HEM content, Fox equation and G–T predictions.

Table 1  
Thermal properties of PEO/PVPh-HEM blends

PVPh-HEM (wt%)	$T_m$ (°C)	$T_g$ (°C)	$\Delta T_g$ (°C)	$\Delta C_p$ ( $\times 10^{-2}$ J/g °C)	$\Delta H_m$ (J/g)	$\chi_{c,blend}$ (%)	$\chi_{c,PEO}$ (%)
0	72	−49	15	2,4	136	72	72
10	70	−45	17	5,3	95	51	56
20	66	−45	14	1,5	77	41	51
30	68	−42	15	3,7	75	40	57
40	64	−30	29	6,5	48	26	43
50	–	−21	51	12,6	–	–	–
60	–	−7	52	11,3	–	–	–
70	–	10	65	13,3	–	–	–
80	–	36	41	9,1	–	–	–
90	–	72	43	11,7	–	–	–
100	–	79	46	12,1	–	–	–

of relaxation processes associated with the glass transition. If the system contains microenvironments caused by dipole–dipole interactions, or hydrogen bonding, then it should undergo relaxation processes with different relaxation times, resulting in broadening of the glass transition. Values of  $\Delta T_g$  in the range of 10–25 °C are expected for semi-crystalline homopolymers, as observed for PEO in Table 1. The blends present  $\Delta T_g$  higher than that of pure PEO, which indicates the presence of a greater number of molecular interactions in the blends and these interacting systems should then undergo different relaxation times. For samples with mass fractions between 70 and 100% in PVPh-HEM, the values of  $\Delta T_g$  reflect that of the non-crystalline pure polymer, whereas for mass fractions between 0 and 30% in PVPh-HEM, these values are very close to that of PEO. This behaviour indicates that the nanostructure of both PVPh-HEM and PEO is affected only for concentrations higher than 30 wt% of each of the components. The higher values of  $\Delta T_g$  found for samples containing 50, 60 and 70 wt% PVPh-HEM indicate that different relaxation processes take place, probably due to changes in the different microenvironments present in the solid.

$\Delta C_p$  values were determined assuming that the baselines before and after the glass transition were parallel.  $\Delta C_p$  is associated with the changes in the degree of freedom in the glass transition, resulting from the free volume changes in this region. Additivity of volume is expected for ideal mixtures and in this case  $\Delta C_p$  reflects only the changes of the conformational arrangement and, consequently, the changes in the entropy of the system. The dependence of  $\Delta C_p$  with composition is expected to be linear, if no strong interactions take place. From Table 1, however, the behaviour of the variation of  $\Delta C_p$  with the blend composition studied in this work reflects clearly the non-additivity of volume (deviations from linearity can be observed for several compositions), which indicates strong intermolecular interactions between the blend components.

From the area of the endothermic peak, associated with the melting of the crystalline phase,  $\Delta H_m$  is evaluated. The values decrease from 136 to 48 J/g, varying with the blend composition from pure PEO to a blend containing 40 wt%

PVPh-HEM. As a dilution effect, a decrease in the value of  $\chi_{c,blend}$  is expected when blending PEO with a non-crystalline polymer. The values of  $\chi_{c,blend}$  vary from 72 (pure PEO) to 26% (40 wt% PVPh-HEM), and  $\chi_{c,PEO}$  from 72 to 43%. For higher compositions of PVPh-HEM, the crystallinity is suppressed. The decrease observed in  $\chi_{c,PEO}$  is an indication that the PEO chains (which is the only crystallizable component) have their crystallinity reduced by the presence of the non-crystalline component.

### 3.2. PLOM

Analysis of the optical photomicrographs (Fig. 3) shows large crystals for the PEO sample and the 90/10 PEO/PVPh-HEM blend. All the blend samples presented smaller crystals than pure PEO and a progressive reduction in the size of the crystals can be seen, being more pronounced for the sample containing 50 wt% PVPh-HEM. For this sample, the dimensions of the crystals seem to be in the limit of the resolution utilized. For samples containing more than 60 wt% PVPh-HEM, there are no crystals that can be seen with the resolution and magnification utilized. Keeping the magnification constant and accompanying the decrease in the size of the crystallites, an increase in the number of nucleation centres per area is observed. This increase in the number of nucleation centres (which can be clearly seen comparing the photomicrographs (a) and (e)) is directly related to a change in the nucleation step of the crystallization kinetics [27].

The results based on DSC and optical microscopy indicate that the crystallinity of the sample is reduced with the addition of PVPh-HEM, which inhibited PEO crystallization, indicating a modification in the kinetics of crystal formation and a depression of the melting point.

### 3.3. FTIR

The FTIR technique is important in blend studies since it allows one to describe specific interactions between polymers, which may play an important role in polymer–polymer miscibility. The knowledge of these interactions in

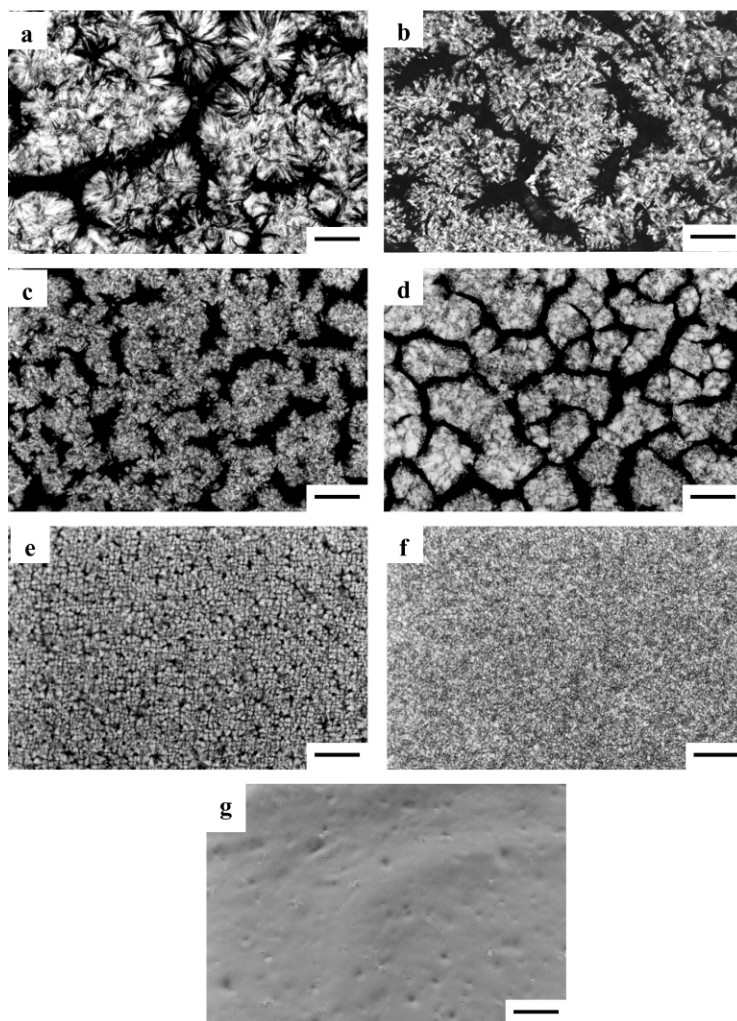


Fig. 3. Optical photomicrographs of the PEO/PVPh-HEM blends. PEO/PVPh-HEM mass ratios: (a) 100/0, (b) 90/10 (c) 80/20, (d) 70/30, (e) 60/40, (f) 50/50, (g) more than 50 wt% PVPh-HEM. Scale bars indicate 0, 5 mm.

a blend will be useful when it is used as a host matrix in a solid electrolyte, since the nanostructure, which is strongly influenced by the specific interactions, is one of the factors that determine the properties of the solid. The enhancement of the ionic conductivity in PEO-based PSE is achieved by decreasing its crystallinity and, especially for PEO blend-based PSE, increasing its homogeneity. In a previous work [28], a PSE based on a PEO blend with poly(methyl vinyl ether–maleic acid) was studied. In the PSE, the dipole–dipole interaction (basic ether oxygen atom of PEO with acidic OH group) in the blend was replaced by an ion–dipole interaction with  $\text{Li}^+$ . This ion–dipole interaction acts as a transient crosslinking and favours the compatibility of the complex systems.

To verify the intermolecular interactions that can play a role in miscibility, determined by the DSC technique, the vibrational spectra of the blends studied in the present work were obtained. In polymeric systems, where there are multiple interactions, vibrational bands such as  $\nu(\text{C}=\text{O})$ ,  $\nu(\text{COC})$  and  $\nu(\text{OH})$  present contributions of spectroscopic free and associated forms. In Fig. 4, the pure PEO and the

blends spectra in selected regions are shown: OH vibrational frequency ( $3800\text{--}3000\text{ cm}^{-1}$ ),  $\text{C}=\text{O}$  stretching ( $1800\text{--}1650\text{ cm}^{-1}$ ) and  $\text{C}-\text{O}-\text{C}$  symmetric stretching ( $1200\text{--}1000\text{ cm}^{-1}$ ). A crystalline PEO phase is confirmed by the presence of the triplet peak of the COC stretching vibration at 1148, 1110, and  $1062\text{ cm}^{-1}$  with a maximum at  $1110\text{ cm}^{-1}$  [29,30]. Changes in the intensity, shape, and position of the COC stretching mode are associated with the interaction between PEO and PVPh-HEM. The shape of the band is not strongly altered for PVPh-HEM concentrations up to 40 wt%, however, a shift to lower wavenumbers in the maximum of the spectra is clearly observed for blends containing up to 30 wt% PVPh-HEM. The broadening of this band for PVPh-HEM concentrations from 50 to 80 wt% is also observed. The intensity of the side bands at 1144 and  $1062\text{ cm}^{-1}$  decrease, due to the decrease of PEO crystallinity in the blends [21], as confirmed by the calculated degree of crystallinity, as previously discussed. Intermolecular interactions can also contribute to the broadening of these bands. For the carbonyl group, two distinct contributions can be clearly observed in the vibrational mode for

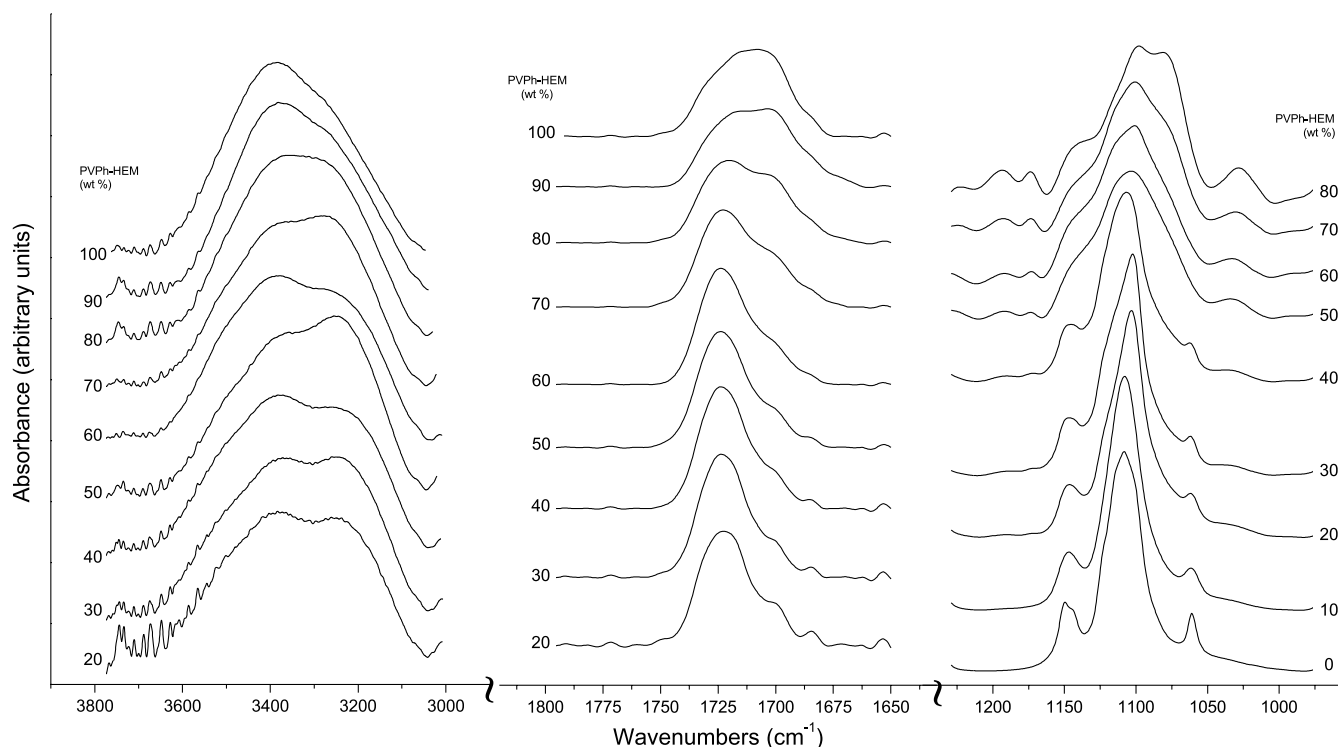


Fig. 4. FTIR spectra of the PEO/PVPh-HEM blends in selected regions: OH vibrational frequency ( $3800\text{--}3000\text{ cm}^{-1}$ ), C=O stretching ( $1800\text{--}1650\text{ cm}^{-1}$ ) and C–O–C symmetric stretching ( $1200\text{--}1000\text{ cm}^{-1}$ ).

all samples, which are attributed to the spectroscopically free and bound carbonyl forms at  $1725$  and  $1705\text{ cm}^{-1}$ , respectively. The maxima of the individual contributions (free and bound) to the bands were found to be almost invariant with the blend composition, and the variation of the spectroscopic fractions with composition is shown in Fig. 5. For the pure PVPh-HEM, the spectroscopically bound form of carbonyl group is predominant, due to the number of hydrogen bond (PVPh-HEM/PVPh-HEM) interactions involving the C=O group. Addition of up to 30 wt%

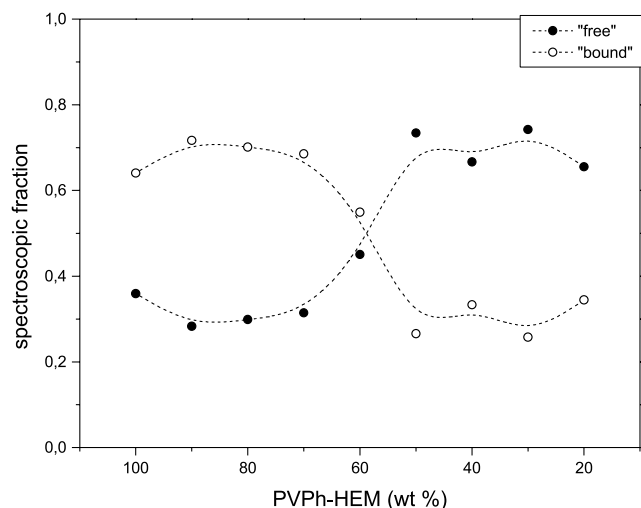


Fig. 5. Spectroscopic fraction of free and bound C=O as a function of PVPh-HEM concentration.

PEO to PVPh-HEM does not affect this ratio. For blends with PEO content higher than 40 wt%, there is an inversion of this ratio, which indicates that the intermolecular (or intramolecular) interactions involving hydroxyl and carbonyl or ether groups (both from PVPh-HEM macromolecules in PVPh-HEM/PVPh-HEM interactions) are replaced by intermolecular interactions involving hydroxyl and ether groups (from PEO in PEO/PVPh-HEM interactions). This assumption is supported by the changes in the shape and position of the C–O–C vibrational mode band and by the analysis of the OH band (Fig. 4). The hydroxyl band was resolved into two distinct contributions, free and bound, following the same approach utilized for the C=O band. The variation of the ratio of the spectroscopically free and bound forms with the blend composition is represented in Fig. 6. The spectroscopically bound form of the hydroxyl group increases monotonically with the addition of PEO to the blend. Hydroxyl groups of PVPh-HEM are probably randomly distributed among an increasing number of ether groups on PEO chains, statistically favouring the formation of the PVPh-HEM/PEO interactions [18]. The decrease in the spectroscopically bound form of C=O (Fig. 5) and the continuous increase in the spectroscopically bound form of OH (Fig. 6) indicate a change in the preferential binding site for hydrogen bonding: from C=O groups in PVPh-HEM-rich blends to oxygen atom (COC) in PEO-rich ones. It is important to note that the continuous increase in spectroscopically bound OH is accompanied by significant changes in COC stretching region for high PEO amounts. These

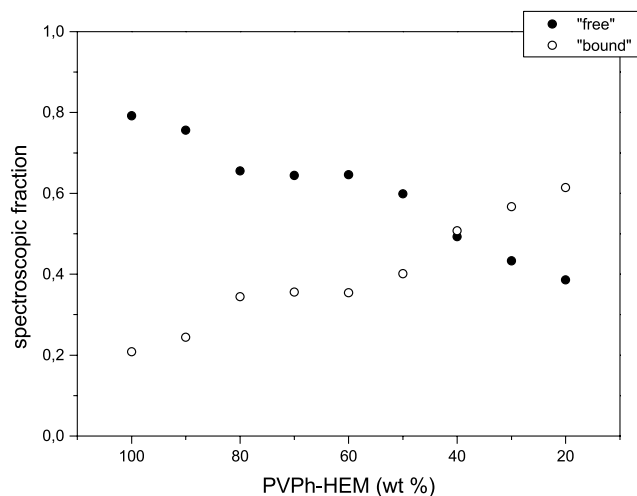


Fig. 6. Spectroscopic fraction of free and bound OH as a function of PVPh-HEM concentration.

interactions induce the solubility and dilution of PVPh-HEM in PEO and favours the miscibility of the blend, as suggested by the DSC study.

As observed in blends of poly(4-vinylphenol) and poly(2-ethoxyethyl methacrylate) [24], the formation of inter-associated systems, i.e. hydrogen bonds involving the phenolic hydrogen and a carbonyl or ether group, is possible for blends of these homopolymers and also should be possible for similar copolymers. The existence of equilibrium between the different forms of associated (or 'bound') and non-associated (or 'free') systems is known to depend on the number of hydrogen bond sites, the volume fraction of the components and the equilibrium constants that describe the competing equilibria within the system. Fig. 7 exhibits some of the possible molecular structures for the present study in three different equilibrium reactions. The equilibrium between the ring and linear forms of the group 2-hydroxyethyl methacrylate is shown in Fig. 7a. The formation of hydrogen bond between the phenolic group and the ether group is represented in Fig. 7b and the equilibrium between two semi-open and one ring forms of two interacting groups 2-hydroxyethyl methacrylate is shown in Fig. 7c. Fig. 8 exhibits two possible molecular structures representing the interaction between PEO and PVPh-HEM. There is spectroscopic evidence for the presence of these last two structures and the mentioned equilibria. In the blends richer in PVPh-HEM, the equilibria represented in Fig. 7 take place and the spectroscopic fractions of either hydroxyl and carbonyl groups indicate the preferential formation of hydrogen bonded self-associated systems, as observed for poly(4-vinylphenol) homopolymer blends with PEO [31]. It is known that the number of different interactions between polymers is determined by the stoichiometry and by the balance of thermodynamic energy terms in the blend, namely enthalpy, combinatorial and non-combinatorial entropy, which in turn are related to the energy of the various interactions and to the backbone

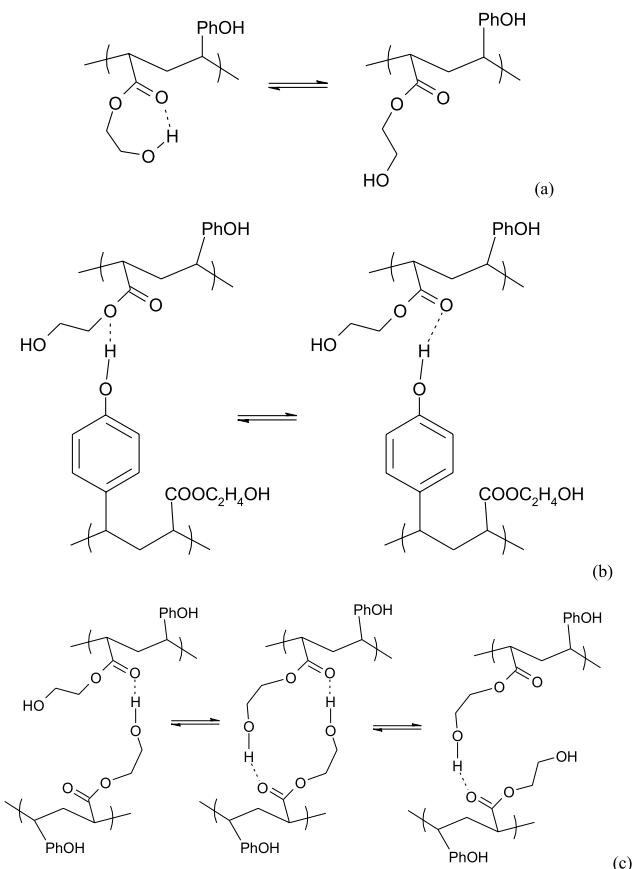


Fig. 7. Molecular structures of PVPh-HEM/PVPh-HEM interacting systems in equilibrium.

and steric hindrance [32]. In the present work, as the PEO concentration in the blend is increased, the formation of systems represented by the structures in Fig. 8 is favoured and, for PEO-rich systems, these are the predominant forms in the blend.

#### 4. Conclusions

The study of PEO/PVPh-HEM blends using DSC showed a single  $T_g$  with a value intermediate between the pure polymers and dependent on the blend composition,

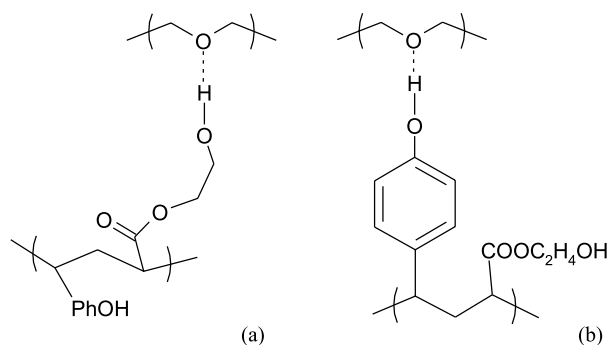


Fig. 8. Molecular structures of PEO/PVPh-HEM interacting systems.

indicating miscibility. From the Fox and G–T models, it can be inferred that, in these blends, there are strong interactions taking place and the solid is quite homogeneous. The presence of PVPh-HEM in the blends decreased the degree of crystallinity and size of the PEO spherulites and depressed the  $T_m$  of the system, which also indicates miscibility. Deconvolution of the FTIR spectra provided experimental evidence of the formation of ‘self-associated’ forms of PVPh-HEM and ‘inter associated’ forms of PEO/PVPh-HEM molecules, via hydrogen bonds.

The PEO/PVPh-HEM blend, which is miscible and homogeneous in the entire range of compositions studied, presents reduced crystallinity and convenient specific interactions for its application as a host in PSE of improved conductivity.

### Acknowledgements

The authors would like to thank the State of Rio de Janeiro Foundation for Research Support (FAPERJ, Grant No. E-26/170414/2000) for partial support of this work and the Brazilian National Research Council (CNPq) for fellowships.

### References

- [1] Acosta JL, Morales E. *J Appl Polym Sci* 1996;60:1185.
- [2] Mastragostino M, Arbizzani C, Meneghelo L, Paraventi R. *Adv Mater* 1996;4:331.
- [3] De Paoli M-A, Zanelli A, Mastragostino M, Rocco AM. *J Electroanal Chem* 1997;435:217.
- [4] Bruce PG, editor. *Solid state electrochemistry*. Cambridge: Cambridge University Press; 1997. p. 106.
- [5] Armand MB. In: McCallum JR, Vincent CA, editors. *Polymer electrolyte reviews*, vol. 1. London: Elsevier; 1989. p. 1.
- [6] Chintapallis FR, Grad B. *Polymer* 1997;38:6189.
- [7] Lee CC, Wright PV. *Polymer* 1982;23:681.
- [8] Xia DW, Smid J. *J Polym Sci Polym Lett* 1984;22:617.
- [9] Zheng S, Huang J, Liu W, Yang X, Guo Q. *Eur Polym J* 1996;32:757.
- [10] Su F, Feng LX, Yang SL. *Appl Chem* 1987;4:40.
- [11] Fish D, Xia DW, Smid S. *Makromol Chem* 1985;6:761.
- [12] Rajendran S, Mahendran O, Mahalingan T. *Eur Polym J* 2002;38:49.
- [13] Choi NS, Park JK. *Electrochim Acta* 2001;46:1453.
- [14] Sajkiewicz P. *Polymer* 2001;46:768.
- [15] Jang GS, Jo NJ, Cho WJ, Ha CS. *J Appl Polym Sci* 2002;83:201.
- [16] Rocco AM, Pereira RP, Felisberti MI. *Polymer* 2001;42:5199.
- [17] Coleman MKM, Moskala EJ. *Polymer* 1983;24:251.
- [18] Berridi MJF, Valero M, Learthum AM, Espi E, Truin J. *Polymer* 1994;34:38.
- [19] Cimmino S. *Makromol Chem* 1990;19:2447.
- [20] Wieckzoreck W, Lipka P, Zukowska G, Wycislik H. *J Phys Chem B* 1998;102:6968.
- [21] Fox TG. *J Appl Bull Am Phys Soc* 1956;1:123.
- [22] Gordon M, Taylor JS. *J Appl Chem* 1952;2:493.
- [23] Woo EM, Mandal TK, Chang LL, Lee SC. *Polymer* 2000;41:6663.
- [24] Hill DJT, Whittaker AK, Wong KW. *Macromolecules* 1999;32:5285.
- [25] Araujo MA, Stadler R, Cantow H-J. *Polymer* 1998;29:2235.
- [26] Casarino P, Vicini S, Pedemonte E. *Thermochim Acta* 2001;372:59.
- [27] Dreezen G, Fang Z, Groeninckx G. *Polymer* 1999;40:5907.
- [28] Rocco AM, Fonseca CP, Pereira RP. *Polymer* 2002;43:3601.
- [29] Li X, Hsu SL. *J Polym Sci, Polym Phys Ed* 1984;22:1331.
- [30] Bailey JrFE, Koleske JV. *Poly(ethylene oxide)*. New York: Academic Press; 1976. p. 115.
- [31] Kuo SW, Chang FC. *Macromolecules* 2001;34:4089.
- [32] Li D, Brisson J. *Polymer* 1998;39:793.